

## Magnetoplasmons in thin films in the Voigt configuration

M. S. Kushwaha and P. Halevi

*Departamento de Física, Instituto de Ciencias, Universidad Autónoma de Puebla, Apartado Postal J-48, Puebla 72570 Mexico*

(Received 19 March 1987)

We have studied the magnetoplasma modes of a thin film, bounded by two dissimilar dielectrics, the applied magnetic field  $\mathbf{B}_0$  being parallel to the interfaces and the waves propagating in a direction perpendicular to  $\mathbf{B}_0$  (Voigt geometry). On the basis of local theory we have derived the exact dispersion relation that governs the propagation characteristics of both surface and bulk (or waveguide) modes. These waves are  $p$  (or TM) polarized and exhibit nonreciprocity with respect to their direction of propagation. An analytic solution for the propagation constant  $q_z(\omega)$  has been found in the nonretarded limit, valid for  $\omega/c \ll |q_z| \ll 1/d$ , where  $d$  is the thickness of the film. In the limit  $|q_z| \rightarrow \infty$  there are two surface modes whose limiting frequencies are given by  $\epsilon_{zz}(\omega) \pm i\epsilon_{yz}(\omega) \text{sgn}(q_z) = -\epsilon_j$ , where  $\epsilon_{ij}(\omega)$  is an element of the dielectric tensor of the semiconductor, and  $\epsilon_1$  and  $\epsilon_3$  are the dielectric constants of the bounding media. Moreover, in the nonretarded limit as  $\mathbf{B}_0$  is increased, the upper mode changes its behavior from monotonically decreasing to monotonically increasing; for a simple model of  $\epsilon_{ij}(\omega)$  this occurs at a critical value of the cyclotron-frequency to plasma-frequency ratio  $\omega_c/\omega_p = [\epsilon_L(\epsilon_L^2/\epsilon_j^2 - 1)]^{-1/2}$ , where  $\epsilon_L$  is the background dielectric constant and, for  $q_z > 0$  ( $q_z < 0$ ) the correct choice is  $j = 3$  ( $j = 1$ ). Then, for a given propagation direction, the upper surface mode degenerates into a horizontal line, i.e., the corresponding group velocity vanishes. We have also applied to the general dispersion relation a thin-film approximation  $\beta d \ll 1$ . This enables us to find an analytic solution in two cases: (1) a very thin semiconducting overlayer on a metallic substrate, giving rise to a splitting in the spectrum in the vicinity of the hybrid cyclotron-plasmon frequency with the creation of a gap; (2) a very thin, unsupported, magnetoplasma film in which case we find four polariton branches.

### I. INTRODUCTION

We have recently embarked on a systematic study of magnetoplasma modes in thin semiconducting films bounded by dissimilar dielectric media.<sup>1</sup> The propagation vector  $\text{Req}$  is parallel to the thin-film structure. In the presence of an applied magnetic field ( $\mathbf{B}_0$ ) there are three basic configurations, namely, (i)  $\mathbf{B}_0$  perpendicular to the surface, (ii)  $\mathbf{B}_0$  parallel to the surface and to the propagation vector  $\text{Req}$  (Faraday configuration), and (iii)  $\mathbf{B}_0$  parallel to the surface and perpendicular to  $\text{Req}$  (Voigt configuration). Of these we have presented a detailed study of the Faraday configuration.<sup>1,2</sup> In the present work we will explore the Voigt configuration (see Fig. 1).

The effect of an externally applied magnetic field ( $\mathbf{B}_0$ ) on surface plasmons in metals and semiconductors in the Voigt configuration has been studied by a number of authors.<sup>3-7</sup> For recent reviews the reader is referred to articles by Halevi<sup>8</sup> and Wallis.<sup>9</sup> Although the application of an applied magnetic field in all the geometries causes various qualitative changes in the behavior characteristic of plasma modes, the Voigt configuration presents some particularly interesting features. For instance, the dispersion relation for surface magnetoplasmons becomes asymmetric with respect to the direction of the wave vector (change of sign), and the dispersion spectrum exhibits a magnetic-field-dependent energy gap.

An important characteristic of the Voigt configuration is that it preserves the TM ( $p$ -polarized) nature of the modes, just as in the absence of  $\mathbf{B}_0$ .

Recently a great deal of attention has been focused on studies of surface plasmons in thin metallic films and multilayered structures. A few workers have studied the propagation range and the lifetime of plasmon polaritons in thin films, in addition to their dispersion characteristics.<sup>10-12</sup> The effect of an applied magnetic field in the Voigt configuration in an unbounded thin film was studied by De Wames and Hall.<sup>13</sup> It will be shown later that their numerical results for the dispersion curves are con-

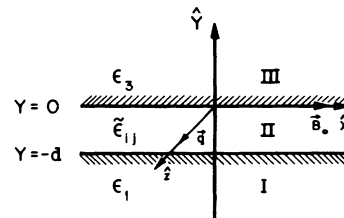


FIG. 1. The schematics of the configuration studied in the present paper. The applied magnetic field  $\mathbf{B}_0$  and the direction of propagation are parallel to the interfaces and perpendicular to each other. We refer to the cases  $\epsilon_1 \neq \epsilon_3$  and  $\epsilon_1 = \epsilon_3$  as the asymmetric and symmetric configurations, respectively.

sistent with the ones that we will present here for the special case of the symmetric configuration. Recently, Sarid<sup>14</sup> has studied surface plasmons in a thin metallic film bounded by two semi-infinite identical semiconductors in the Voigt configuration. This author has shown that the application of a magnetic field modifies the symmetry of the (otherwise identical) bounding media, as a result of which both modes, particularly the long-range one, experience a dramatic decrease in their propagation lengths. The configuration considered by Sarid<sup>14</sup> corresponds to the symmetric strip line, a well-established magnetospectroscopic technique in the submillimeter range.<sup>15</sup> There also exist several experimental works that utilize the attenuated-total-reflection (ATR) method in the far infrared,<sup>16-18</sup> as well as in the submillimeter<sup>19</sup> region of the spectrum. This method is particularly suitable in the Voigt geometry because of the simple polarization (TM) of the magnetoplasma modes as compared with configurations that involve other directions of the magnetic field.

In the present work we will study the dispersion characteristics of magnetoplasma modes propagating along a lossy thin semiconducting film bounded by two dissimilar dielectric media; the waves propagate in a direction perpendicular to the applied magnetic field, itself parallel to the surface. It should be pointed out that in the absence of an applied magnetic field, all the three media constituting the geometry depicted in Fig. 1 are isotropic.

The remainder of the paper is organized as follows. In Sec. II we present the derivation of the general dispersion relation. In Sec. III we study this relation in the nonretarded limit ( $c \rightarrow \infty$ ). The slope of the upper surface mode exhibits an interesting dependence on  $\mathbf{B}_0$ ; this behavior is also analyzed in Sec. III. In Sec. IV we subject our general dispersion relation to an approximation valid for very thin films and investigate two cases of interest: (A) surface polaritons modified by a magnetized overlayer, and (B) a magnetized film bounded by two identical dielectric media. It is worthwhile mentioning that our accomplishment lies in presenting analytic solutions and thus physical insight into a rather complex problem. The detailed numerical calculations are deferred to a future work.

## II. DERIVATION OF GENERAL DISPERSION RELATION

We consider a semiconducting film (medium II) of finite thickness characterized by a dielectric tensor  $\tilde{\epsilon}$  which is assumed to be independent of the propagation vector ( $\mathbf{q}$ ). The semiconducting film is asymmetrically bounded by two semi-infinite dielectric media I and III, their dielectric constants being  $\epsilon_1$  and  $\epsilon_3$ , respectively. The magnetostatic field ( $\mathbf{B}_0$ ) is assumed to be oriented parallel to the interfaces which are perpendicular to the  $\hat{y}$  axis. The three media constitute the geometry shown in Fig. 1. The direction of  $\mathbf{B}_0$  is parallel to the  $\hat{x}$  axis and perpendicular to  $\mathbf{q}$  which is parallel to the  $\hat{z}$  axis, i.e., we are concerned with the Voigt configuration.

For the derivation of the dispersion relation we resort

to Maxwell's curl field equations. After eliminating the magnetic field variable ( $\mathbf{H}$ ), we obtain the following wave equation for the macroscopic electric field ( $\mathbf{E}$ ):

$$\nabla \times (\nabla \times \mathbf{E}) - q_0^2 \tilde{\epsilon} \cdot \mathbf{E} = 0, \quad (1)$$

where  $q_0 = \omega/c$  is the vacuum wave vector,  $\omega$  being the angular wave frequency, and  $c$  the velocity of light in vacuum. We assume that spatial and temporal dependence of the fields is of the form  $\sim e^{i(\mathbf{q} \cdot \mathbf{r} - \omega t)}$ . In the present configuration ( $\mathbf{B}_0 \parallel \mathbf{x}$ ) the dielectric tensor is simplified by the symmetry requirements that  $\epsilon_{yy} = \epsilon_{zz}$ ,  $\epsilon_{zy} = -\epsilon_{yz}$ , and  $\epsilon_{xy} = \epsilon_{yx} = \epsilon_{xz} = \epsilon_{zx} = 0$ . Consequently, Eq. (1) may be rewritten as follows:

$$\begin{pmatrix} q_0^2 \epsilon_{xx} - q_y^2 - q_z^2 & 0 & 0 \\ 0 & q_0^2 \epsilon_{zz} - q_z^2 & q_0^2 \epsilon_{yz} + q_y q_z \\ 0 & -q_0^2 \epsilon_{yz} + q_y q_z & q_0^2 \epsilon_{zz} - q_y^2 \end{pmatrix} \begin{pmatrix} E_x \\ E_y \\ E_z \end{pmatrix} = 0. \quad (2)$$

Equation (2) is a set of three linear homogeneous equations satisfied by the electric field in the dispersive anisotropic semiconducting medium II. The same set of three equations also give valid solutions of Maxwell's equations in the isotropic media I and III, if we just take  $\epsilon_{yz} = 0$  and  $\epsilon_{yy} = \epsilon_{zz} = \epsilon_i$  ( $i \equiv 1$  and  $3$ , respectively, for media I and III). The nontrivial solution of such a set of three linear equations requires the vanishing of the determinant of the coefficients. As such one obtains

$$-q_y^2 \equiv \beta^2 = q_z^2 - q_0^2 (\epsilon_{zz} + \epsilon_{yz}^2 / \epsilon_{zz}), \quad (3)$$

in the semiconducting medium [note that  $(q_y^2 + q_z^2) = q_0^2 (\epsilon_{zz} + \epsilon_{yz}^2 / \epsilon_{zz})$  is simply the dispersion relation for the bulk modes in the Voigt geometry] and

$$-q_y^2 \equiv \alpha_i^2 = q_z^2 - q_0^2 \epsilon_i, \quad i \equiv 1, 3 \quad (4)$$

in the dielectric media. In Eqs. (3) and (4)  $\beta$  ( $= \pm i q_y$ ) refers to the decay constant in medium II and  $\alpha_i$  ( $= \pm i q_y$ ) to those in media I ( $i = 1$ ) and III ( $i = 3$ ).

Because of the TM character of the magnetoplasma waves, we choose to solve the wave field equations in terms of the nonvanishing transverse magnetic field component  $H_x$ . We write the field distributions in the three media in the form (see Fig. 1)

$$H_x(r, t) = H_x(y) e^{i(q_z z - \omega t)}, \quad (5)$$

where  $H_x(y)$  for regions I ( $y \leq -d$ ), II ( $-d \leq y < 0$ ), and III ( $y \geq 0$ ) is expressed as follows:

$$H_x^I(y) = H_x^I e^{\alpha_1 y}, \quad (6)$$

$$H_x^{II}(y) = H_{x1} e^{-\beta y} + H_{x2} e^{\beta y}, \quad (7)$$

and

$$H_x^{III}(y) = H_x^{III} e^{-\alpha_3 y}. \quad (8)$$

Analogous solutions can be written for the electric field  $\mathbf{E}$  in the three regions.

Since we are considering TM waves, the nonvanishing field components are  $H_x$ ,  $E_y$ , and  $E_z$ . It is noteworthy

that  $E_x \neq 0$  and  $E_y = E_z = 0$  (i.e.,  $-q_y^2 = q_z^2 - q_0^2 \epsilon_{xx}$ ) would lead to TE (*s*-polarized) waves. However, carriers drifting parallel to the applied field do not experience a magnetic force. The situation is identical to the field-free case, and will not be pursued further. The boundary conditions in the present configuration are the continuity of the tangential field components  $H_x$  and  $E_z$ . Using Maxwell's curl field equations and Eq. (2) we can express  $E_z$  in terms of  $H_x$  in the three media. Employing the boundary conditions at the two interfaces ( $y=0$  and  $y=-d$ ) yields the following relations:

$y=0$ :

$$H_x^{\text{III}} = H_{x1} + H_{x2}, \quad (9)$$

$$\frac{\alpha_3}{\epsilon_3} H_x^{\text{III}} = \frac{k^2}{(\beta \epsilon_{zz} - i q_z \epsilon_{yz})} H_{x1} + \frac{k^2}{(-\beta \epsilon_{zz} - i q_z \epsilon_{yz})} H_{x2}, \quad (10)$$

$y=-d$ :

$$H_x^{\text{I}} e^{-\alpha_1 d} = H_{x1} e^{\beta d} + H_{x2} e^{-\beta d}, \quad (11)$$

$$-\frac{\alpha_1}{\epsilon_1} H_x^{\text{I}} e^{-\alpha_1 d} = \frac{k^2}{(\beta \epsilon_{zz} - i q_z \epsilon_{yz})} H_{x1} e^{\beta d} + \frac{k^2}{(-\beta \epsilon_{zz} - i q_z \epsilon_{yz})} H_{x2} e^{-\beta d}, \quad (12)$$

where

$$k^2 = q_z^2 - q_0^2 \epsilon_{zz}. \quad (13)$$

Equations (9)–(12) are four homogeneous equations in terms of four unknowns— $H_x^{\text{I}}$ ,  $H_x^{\text{III}}$ ,  $H_{x1}$ , and  $H_{x2}$ . This system of equations admits a nontrivial solution only if the determinant of the coefficients vanishes. This leaves us, after some algebra, with the following relation:

$$[\alpha_1 \alpha_3 (\epsilon_{zz}^2 + \epsilon_{yz}^2) + k^2 \epsilon_1 \epsilon_3 + i q_z \epsilon_{yz} (\alpha_3 \epsilon_1 - \alpha_1 \epsilon_3)] \tanh(\beta d) + \beta \epsilon_{zz} (\alpha_3 \epsilon_1 + \alpha_1 \epsilon_3) = 0. \quad (14)$$

Equation (14) is the dispersion relation for the TM magnetoplasma waves in the Voigt configuration. One notes immediately from Eq. (14) that the dispersion relation is nonreciprocal—i.e., positive and negative values of the wave vector  $q_z$  are not equivalent.

We are interested in the propagating-wave solutions of Eq. (14), i.e.,  $q_z$  must be real in the absence of damping. Then  $\alpha_1$  and  $\alpha_3$ , given in Eq. (4), are either real or pure imaginary. The latter case of certain interest in waveguide theory ("substrate modes" and "air modes").<sup>20</sup> In the present work we will limit our attention to solutions which decay exponentially away from both the interfaces of the film. Such solutions are characterized by both  $\alpha_1$  and  $\alpha_3$  being real and positive. The real magnetoplasma modes with real  $q_z$ ,  $\alpha_1$ , and  $\alpha_3$  may be further classified according to the nature of  $\beta$ , given by Eq. (3). Depending upon the spectral range in the  $(\omega - q_z)$  plane the following possibilities may arise.

(i)  $\beta$  is real and positive [we may always choose the

positive root of  $\beta$ , in view of our field solutions, Eq. (7)]. This corresponds to polariton or surface modes decaying away from both the interfaces, inside as well as outside the film.

(ii)  $\beta$  is pure imaginary (one may choose  $\text{Im}\beta > 0$ ). These are waveguide (WG) or bulk modes with an oscillatory field dependence inside the film.

This classification of the modes into polaritons and waveguide modes is valid only if the dissipation is neglected (i.e., the carrier collisional frequency  $\nu=0$ ). With finite absorption ( $\nu \neq 0$ )  $q_z$ ,  $\alpha_1$ ,  $\alpha_3$  are  $\beta$  are, of course, all complex quantities. In the present paper we will assume  $\nu=0$ , where  $\epsilon_{zz}$  and  $\epsilon_{xx}$  are real and  $\epsilon_{yz}$  is pure imaginary. Effects of absorption will be dealt with in a future publication.

We have checked Eq. (14) by subjecting it to various special limits, viz.,  $d=0$ ,  $d \rightarrow \infty$ , and  $\mathbf{B}_0=0$ . It is found that within these limits our general dispersion relation reproduces exactly the results previously reported for a single interface ( $\mathbf{B}_0 \neq 0$ ) (Refs. 3, 4, 6, 8, and 9) and for a thin film with<sup>13</sup> and without<sup>11,21</sup> an applied magnetic field.

Our numerical results are based on the following model for the dielectric tensor elements ( $\epsilon_{ij}$ ) relevant to our geometry (Fig. 1):

$$\begin{aligned} \epsilon_{yy} = \epsilon_{zz} = \epsilon_L + \frac{\omega_p^2}{(\omega_c^2 - \omega^2)}, \\ \epsilon_{yz} = -i \frac{\omega_p^2 \omega_c}{\omega(\omega_c^2 - \omega^2)}, \\ \epsilon_{xx} = \epsilon_L - \frac{\omega_p^2}{\omega^2}, \end{aligned} \quad (15)$$

where  $\omega_p = (4\pi n e^2 / m^*)^{1/2}$  and  $\omega_c = e |\mathbf{B}_0| / m^* c$  are, respectively, the unscreened plasma frequency and cyclotron frequency;  $e$ ,  $m^*$ , and  $n$  being, respectively, the electronic charge, effective mass, and free-carrier concentration in the semiconducting film (region II in Fig. 1). However, it should be pointed out that most of the analytic results in the present paper are independent of any particular model. For instance, we can always incorporate the effects of the carrier collisional frequency (in order to account for the absorption) and the frequency dependence of the background dielectric constant ( $\epsilon_L$ ) which, in other words, allows the coupling of magnetoplasmons to optical phonons.

### III. NONRETARDED LIMIT

In the nonretarded (NR) limit we assume  $|q_z| \gg q_0$  which is, mathematically, equivalent to taking  $c \rightarrow \infty$ . Then  $\alpha_1 = \alpha_3 = k = \beta = |q_z|$ , since by definition  $\alpha_i$  ( $i=1, 3$ ) and  $\beta$  are positive. In order to account for the nonreciprocity of the dispersion relation we substitute  $q_z = |q_z| \text{sgn} q_z$  in Eq. (14). Consequently it becomes

$$[(\epsilon_{zz}^2 + \epsilon_{yz}^2 + \epsilon_1 \epsilon_3) + \text{sgn}(q_z)(i \epsilon_{yz})(\epsilon_1 - \epsilon_3)] \times \tanh(|q_z| d) + \epsilon_{zz}(\epsilon_1 + \epsilon_3) = 0. \quad (16)$$

This is the dispersion relation for the magnetoplasma po-

laritons in the NR limit for an arbitrary thickness of the semiconducting film. The presence of the off-diagonal element  $\epsilon_{yz}$  indicates that the dynamical Hall effect plays a significant role even in the NR limit—unlike the case of the Faraday configuration.<sup>1</sup> On the other hand, the element  $\epsilon_{xx}$  has dropped out. We will analyze Eq. (16) in the following two cases.

*The case  $|q_z|d \rightarrow \infty$ .* First we consider the case  $|q_z| \gg 1/d$ ; taken together with  $|q_z| \gg q_0$  this implies that  $|q_z| \rightarrow \infty$ . As a result, Eq. (16) assumes the form

$$\epsilon_{zz}^2 + \epsilon_{yz}^2 + \epsilon_1\epsilon_3 + \text{sgn}(q_z)(i\epsilon_{yz})(\epsilon_1 - \epsilon_3) + \epsilon_{zz}(\epsilon_1 + \epsilon_3) = 0. \quad (17)$$

A simple factorization of the left-hand side of Eq. (17) leads to two possible solutions:

$$\epsilon_{zz} + \text{sgn}(q_z)(i\epsilon_{yz}) + \epsilon_3 = 0, \quad (18a)$$

and

$$\epsilon_{zz} - \text{sgn}(q_z)(i\epsilon_{yz}) + \epsilon_1 = 0. \quad (18b)$$

In the case  $\mathbf{B}_0=0$  and hence  $\epsilon_{yz}=0$  and  $\epsilon_{zz}=\epsilon(\omega)$ , Eq. (18) reduces to  $\epsilon(\omega)=-\epsilon_i$  ( $i=1,3$ ) as it should be.<sup>22</sup> Equations (18) represents the asymptotic solutions corresponding, respectively, to the II-III and II-I interfaces. Substituting  $\epsilon_{zz}$  and  $\epsilon_{yz}$  from Eq. (15) in Eqs. (18) gives, after some algebraic steps,

$$\omega_{s+} = \left[ \frac{\omega_c^2}{4} + \frac{\omega_p^2}{\epsilon_L + \epsilon_3} \right]^{1/2} + \frac{1}{2}\text{sgn}(q_z)\omega_c, \quad (19a)$$

and

$$\omega_{s-} = \left[ \frac{\omega_c^2}{4} + \frac{\omega_p^2}{\epsilon_L + \epsilon_1} \right]^{1/2} - \frac{1}{2}\text{sgn}(q_z)\omega_c. \quad (19b)$$

Equations (19) imply that there are two asymptotic solutions (corresponding to  $q_z \rightarrow \pm\infty$ ) for each of the two interfaces in the NR limit. Equations (19), for  $\epsilon_1=\epsilon_3=1$ , reduce to Eq. (5) of DeWames and Hall<sup>13</sup> for the symmetric configuration. It is to be noted that the two asymptotic modes corresponding to a given interface are separated by  $|\omega_c|$ . In the special case when  $\mathbf{B}_0=0$ , Eqs. (19) give the solution  $\omega=\omega_p(\epsilon_L + \epsilon_i)^{-1/2}$ ,  $i=1$  or  $3$ , which is the same as Eq. (24) in Ref. (9).

*The case  $|q_z|d \ll 1$ .* In the NR limit this assumption is equivalent to  $q_0 \ll |q_z| \ll 1/d$ . As a result, Eq. (16) reduces to

$$|q_z|d = - \frac{\epsilon_{zz}(\epsilon_1 + \epsilon_3)}{[\epsilon_{zz}^2 + \epsilon_{yz}^2 + \epsilon_1\epsilon_3 + \text{sgn}(q_z)(i\epsilon_{yz})(\epsilon_1 - \epsilon_3)]}. \quad (20)$$

Because the NR limit requires that  $|q_z| \gg q_0$ , this result holds only for very thin films, namely  $q_0d \ll 1$ . In what follows, two different cases regarding the dispersion relation, Eq. (20), have been analyzed.

(i)  $\epsilon_1 > \epsilon_3 \geq 1$ . For  $q_z=0$ , we must have either  $\epsilon_{zz}=0$  or  $\epsilon_{yz} \rightarrow \infty$ , as may be seen from Eq. (20). This gives, re-

spectively, for the upper and the lower modes

$$\omega = \omega_H \quad \text{and} \quad \omega = 0 \quad \text{for} \quad q_z = 0, \quad (21)$$

where

$$\omega_H = (\omega_c^2 + \omega_p^2/\epsilon_L)^{1/2} \quad (22)$$

is the well-known hybrid cyclotron-plasma frequency at which  $\epsilon_{zz}$  vanishes. Note that the other pole of  $\epsilon_{yz}(\omega)$ , namely  $\omega_c$ , is also a pole of  $\epsilon_{zz}$ ; then it is not difficult to show that right-hand side of Eq. (20) is finite. One should not equate the denominator of Eq. (20) to zero while looking for the asymptotic frequencies, because we know that the correct asymptotic frequencies are given by Eqs. (19). The apparent discrepancy is hardly surprising since the present approximation is limited to  $|q_z| \ll 1/d$ . Similarly, Eq. (21) does not give true values of  $\omega(q_z \rightarrow 0)$  because we must satisfy  $|q_z| \gg q_0$ .

We have computed  $q_z$  as a function of  $\omega$ , Eq. (20), with the choice of the following parameters:  $\epsilon_L=15.7$ ,  $\epsilon_1=11.683$ ,  $\epsilon_3=1.0$ , and  $\omega_c/\omega_p=0.5$ . These values specify our layered structure (Fig. 1) as made up of a Si-glass substrate (region I), an InSb film (region II), and air (region III). The numerical results in terms of dimensionless variables are shown in Fig. 2. The two curves, represented by solid lines, are the magnetoplasma analogs of the Fuchs-Kliwer modes and give valid solutions provided that  $q_0 \ll |q_z| \ll 1/d$ . For both directions of propagation the lower mode starts at the origin, while the upper mode starts at  $\omega=\omega_H$  as expected by Eq. (21). As  $\omega$  increases we observe a marked difference in behav-

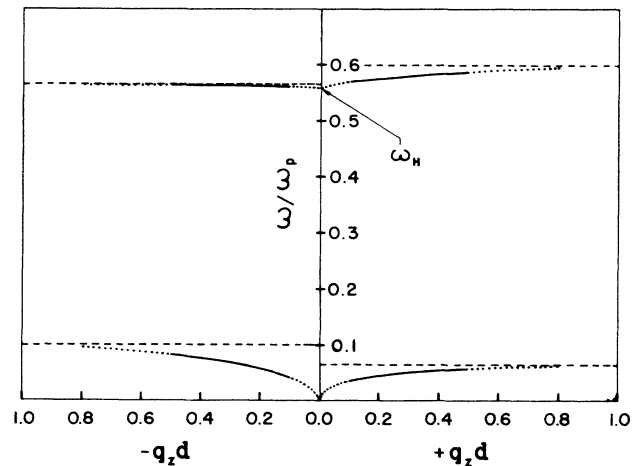


FIG. 2. The normalized frequency  $\omega/\omega_p$  vs normalized propagation constant  $q_z d$  in the nonretarded limit for the asymmetric configuration. The two branches (solid lines) for  $q_z > 0$  and  $q_z < 0$  are solutions of Eq. (20) which correspond to the assumption that  $q_0 \ll |q_z| \ll 1/d$ . The dotted lines indicate that our approximations fail for very small and for very large values of  $|q_z|$ . The asymptotic limits  $|q_z| \rightarrow \infty$  are indicated by dashed lines. The parameters used are  $\epsilon_1=11.683$ ,  $\epsilon_3=1.0$ ,  $\epsilon_L=15.7$ , and  $\omega_c/\omega_p=0.5$ . This corresponds to an InSb film on a Si substrate in the far infrared.

ior for  $q_z > 0$  and  $q_z < 0$ . The asymptotic limits (dashed lines) for the lower and upper modes are given by Eqs. (19b) and (19a), respectively, if  $q_z > 0$ , and the other way round if  $q_z < 0$ . It is worthwhile pointing out that the correct asymptotic limits, given by Eqs. (19), are *almost* the same as those obtained (incorrectly) by equating the denominator of Eq. (20) to zero. This is because the last term in Eq. (17) is negligible as compared with the algebraic sum of the other terms in the regions of both the upper and the lower modes. Actually it seems that the upper branch in Fig. 2 approximates very well the exact behavior provided that  $\omega_c^2/\omega_p^2 \gg 1/\epsilon_L^3$  which is satisfied for all but extremely low magnetic fields. Since, in the NR limit, the decay constants  $\alpha_1$ ,  $\alpha_3$ , and  $\beta$  are all given by  $|q_z|$ , both modes correspond to polaritons bounded to the interfaces.

In Fig. 2 the upper polariton mode starts at  $\omega = \omega_H$  and reaches the asymptotic limits  $\omega_{s+}$  [for  $q_z > 0$ , Eq. (19a)] and  $\omega_{s-}$  [for  $q_z < 0$ , Eq. (19b)]. Because these frequencies are always greater than  $\omega_H$  the upper (as well as the lower) polariton branch is monotonously increasing for  $|q_z| \gg q_0$ . In this aspect the behavior of the upper mode differs from that of the upper Fuchs-Kliwer mode<sup>22</sup> ( $\mathbf{B}_0 = 0$ ) and the corresponding one in the Faraday geometry,<sup>1</sup> in which cases the group velocity ( $V_g$ ) is negative for sufficiently large wave vectors. This suggests that there exists a critical value of the magnetic field at which  $V_g$  of this (upper) mode changes sign from negative to positive.

We note that Eq. (20) is satisfied, for an arbitrary value of  $q_z$  (and  $d$ ), if

$$\omega = \omega_H = \begin{cases} \omega_{s+}, & q_z > 0 \\ \omega_{s-}, & q_z < 0. \end{cases} \quad (23)$$

Solving the last equality we get

$$\frac{\omega_c}{\omega_p} = \frac{\epsilon_3}{[\epsilon_L(\epsilon_L^2 - \epsilon_3^2)]^{1/2}} \equiv \frac{\omega_c^+}{\omega_p}, \quad \text{for } q_z > 0, \quad (24)$$

and

$$\frac{\omega_c}{\omega_p} = \frac{\epsilon_1}{[\epsilon_L(\epsilon_L^2 - \epsilon_1^2)]^{1/2}} \equiv \frac{\omega_c^-}{\omega_p}, \quad \text{for } q_z < 0. \quad (25)$$

We conclude that for the critical values of the magnetic field, given by Eqs. (24) and (25), one side of the upper polariton branch degenerates into a horizontal line  $\omega = \omega_H$ , i.e., for this side of the branch  $V_g = 0$ . Therefore it seems that  $\omega_c < \omega_c^\pm$  and  $\omega_c > \omega_c^\pm$  will lead to negative and positive group velocities, respectively. The numerical values of  $\omega_c^+$  and  $\omega_c^-$ , for the parameters used in the present work, are such that  $\omega_c^+/\omega_p = 0.01611$  and  $\omega_c^-/\omega_p = 0.28112$ .

We have used the aforesaid critical values of the magnetic field to calculate the dispersion curves for this asymmetric case, Eq. (20). The other material parameters used for this purpose were the same as those used in Fig. 2. The numerical results in terms of the dimensionless variables are shown in Fig. 3. The flat (solid) lines designated as  $s_+$  and  $s_-$ , respectively, refer to  $\omega_H = \omega_{s+}$ , for  $q_z > 0$ , and  $\omega_H = \omega_{s-}$ , for  $q_z < 0$ . It is evi-

dent from the figure that the behavior of the lower surface mode is unchanged.

Equations (23)–(25) may be readily generalized for an arbitrary model of  $\epsilon_{ij}(\omega, \mathbf{B}_0)$ . The corresponding equations are

$$\epsilon_{zz}(\omega, \mathbf{B}_0) = 0, \quad (23')$$

$$\epsilon_{yz}(\omega, \mathbf{B}_0) = i\epsilon_3 \text{sgn}(q_z), \quad (24')$$

$$\epsilon_{yz}(\omega, \mathbf{B}_0) = -i\epsilon_1 \text{sgn}(q_z). \quad (25')$$

Equations (23') and (24'), and also equations (23') and (25'), when solved simultaneously, give the critical value (or values) of  $\mathbf{B}_0$  such that certain polariton branches degenerate into lines  $\omega = \text{const}$ , also given by the solutions of the above equations. These solutions are characterized by vanishing group velocities.

Because this behavior is independent of the film thickness, it is also valid for  $d \rightarrow \infty$ , that is, for a surface. No need to say, for  $|q_z| \sim q_0$ , when retardation is important, Eq. (20) is *not* a solution [of Eq. (14)] and, for such values of the wave vector, the group velocity does not vanish in general.

(ii)  $\epsilon_1 = \epsilon_3 = \epsilon_0$  (say). In this symmetric configuration, Eq. (20) assumes the form

$$|q_z|d = -\frac{2\epsilon_0\epsilon_{zz}}{\epsilon_{zz}^2 + \epsilon_{yz}^2 + \epsilon_0^2}. \quad (26)$$

One notes immediately that in this case the dispersion relation is reciprocal.

We have calculated the frequency spectrum, Eq. (26), using  $\epsilon_0 = 1.0$  (unsupported film) with the rest of the pa-

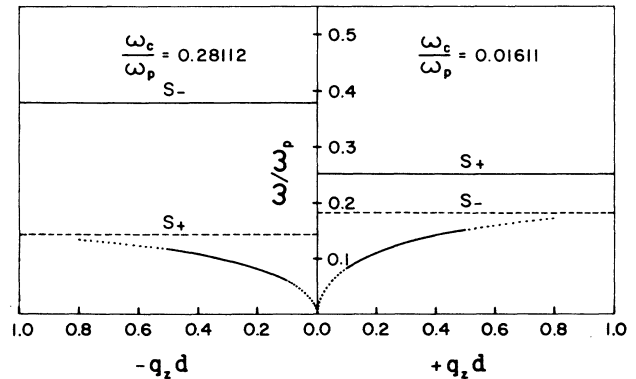


FIG. 3. The dispersion curves in the nonretarded limit for the critical values of the magnetic field, Eqs. (24) and (25), at which the group velocity of the upper polariton mode vanishes. Apart from  $\omega_c/\omega_p = 0.01611$  and  $0.28112$ , respectively, for  $q_z > 0$  and  $q_z < 0$ , the other parameters are the same as in Fig. 2. The horizontal solid lines designated as  $s_+$  and  $s_-$ , respectively, for  $q_z > 0$  (at  $\omega/\omega_p = 0.252891$ ) and  $q_z < 0$  (at  $\omega/\omega_p = 0.377787$ ) are the polariton modes for which  $V_g = 0$ . The horizontal dashed lines designated as  $s_-$  and  $s_+$ , respectively, for  $q_z > 0$  and  $q_z < 0$ , are the asymptotic limits for the lower dispersive (polariton) mode.

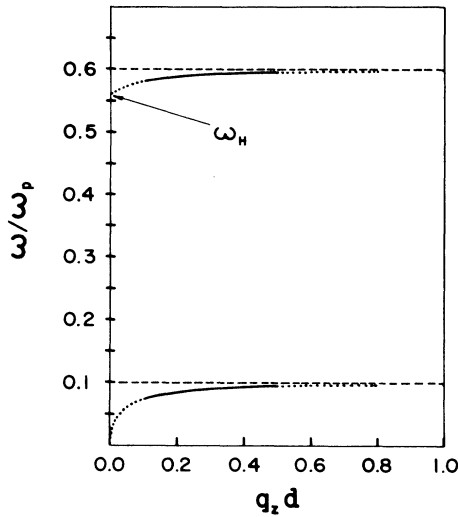


FIG. 4. As in Fig. 2, for the symmetric configuration,  $\epsilon_1 = \epsilon_3 = 1.0$ ; that is, an unsupported InSb film. The two branches (solid lines) are the solutions of Eq. (26). This case is reciprocal.

rameters being the same as stated in case (i). The numerical results for  $\omega/\omega_p$  vs  $q_z d$  are plotted in Fig. 4. The solid curves indicate the dispersive (ordinary) surface modes and the dashed lines stand for the asymptotic limits, for  $\epsilon_1 = \epsilon_3 = 1$  in Eqs. (19). The lower mode starts at the origin and approaches an asymptotic limit at a

frequency specified by Eq. (19b). The upper mode starts at  $\omega = \omega_H$  and approaches an asymptotic limit given by Eq. (19a). It may be noted that, like case (i), the asymptotic limits, correctly given by Eqs. (19), are *almost* the same as those given (incorrectly) by the denominator of the right-hand side of Eq. (26) equated to zero. This behavior is a consequence of a large ratio of  $\epsilon_L$  to  $\epsilon_0 (= 1.0)$ . The noteworthy difference between the asymmetric and symmetric cases can be attributed to the reciprocity in the latter case.

In the symmetric configuration, too, the slope of the upper polariton mode changes from negative to positive as we increase the magnetic field. By Eqs. (24) and (25) this happens when

$$\frac{\omega_c}{\omega_p} = \frac{\epsilon_0}{[\epsilon_L(\epsilon_L^2 - \epsilon_0^2)]^{1/2}}$$

for both directions of propagation. For this value of  $\omega_c/\omega_p$  the group velocity of the upper polariton vanishes in the nonretarded limit.

#### IV. APPROXIMATE DISPERSION RELATIONS FOR VERY THIN FILMS

In this section we invoke a thin-film approximation (TFA)

$$\tanh(\beta d) \simeq \beta d. \quad (27)$$

With this approximation the general dispersion relation, Eq. (14), assumes the form

$$\epsilon_{zz}(\alpha_3 \epsilon_1 + \alpha_1 \epsilon_3) + d[\alpha_1 \alpha_3 (\epsilon_{zz}^2 + \epsilon_{yz}^2) + k^2 \epsilon_1 \epsilon_3 + |q_z| \operatorname{sgn}(q_z)(i \epsilon_{yz})(\alpha_3 \epsilon_1 - \alpha_1 \epsilon_3)] = 0. \quad (28)$$

We will analyze Eq. (28) in two different cases of interest.

##### A. Surface polaritons modified by magnetized overlayer

In this case we assume that medium III is air ( $\epsilon_3 = 1.0$ ) and that medium I is surface-wave active (i.e.,  $\epsilon_1 < 0$ ). We use an ansatz<sup>21</sup>

$$q_z^2 = q_0^2 \frac{\epsilon_1}{1 + \epsilon_1} + K_1^2 \quad (29)$$

for a film of small thickness  $d$ . In the limit  $d \rightarrow 0$ ,  $K_1^2$  must vanish and we are left with the surface plasmon-polariton dispersion relation. For very small but finite  $d$ , we expect that  $K_1^2$  is proportional to some power of  $d$ . Using Eq. (4) and treating  $K_1^2$  as a very small quantity, we calculate  $\alpha_1$ ,  $\alpha_3$ , and  $K$  (see Appendix C in Ref. 1). Substituting in Eq. (28) and neglecting the terms proportional to  $K_1^2$  (and higher-order ones) in the coefficient of  $d$  results

$$K_1^2 = - \frac{2i(q_0^3 d) \epsilon_1^2}{\epsilon_{zz}(1 + \epsilon_1)^{5/2}(1 - \epsilon_1)} [(\epsilon_1 - \epsilon_{zz})(1 - \epsilon_{zz}) + \epsilon_{yz}^2 + 2 \operatorname{sgn}(q_z) \epsilon_{yz} \epsilon_1^{1/2}]. \quad (30)$$

Substituting  $K_1^2$  in Eq. (29) yields

$$|q_z| \simeq q_0 \left[ \left( \frac{\epsilon_1}{1 + \epsilon_1} \right)^{1/2} - \frac{i(q_0 d) \epsilon_1^{3/2}}{\epsilon_{zz}(1 + \epsilon_1)^2(1 - \epsilon_1)} [(\epsilon_1 - \epsilon_{zz})(1 - \epsilon_{zz}) + \epsilon_{yz}^2 + 2 \operatorname{sgn}(q_z) \epsilon_{yz} \epsilon_1^{1/2}] \right]. \quad (31)$$

We note that  $-i \epsilon_1^{3/2} = -i(-|\epsilon_1|)(-i|\epsilon_1|)^{1/2} = |\epsilon_1|^{3/2}$ , so the right-hand side of Eq. (31) is a real quantity. Furthermore, a consideration of the behavior of  $q_y$  and  $q_z$  for  $\epsilon_1(\omega) < 0$  dictates the choices  $\operatorname{Im} \epsilon_1^{1/2} < 0$

and  $\operatorname{Im}(1 + \epsilon_1)^{1/2} < 0$ . An inspection of Eq. (31) reveals that the propagation constant is linear (to the lowest order) in  $d$ . Equation (31) is a good approximation provided that  $q_0 d \ll 1$ . In the special case that  $\mathbf{B}_0 = 0$ , Eq. (31)

reduces to Eq. (3) of López-Ríos<sup>10</sup> provided that  $\epsilon_0$ , the dielectric constant of medium III in his notation, is equal to one.

We have calculated the dispersion curve corresponding to Eq. (31) using the parameters  $\epsilon_L = 15.7$ ,  $\omega_c/\omega_p = 0.5$ , and  $\omega_p d/c = 2\pi \times 10^{-2}$  (for  $d = 2 \mu\text{m}$  this corresponds to  $\omega_p = 1.50 \text{ THz}$ ) and the magnetoplasma model as specified in Eq. (15). For the metallic substrate we assume a simple model<sup>23</sup>  $\epsilon_1 = 1 - \omega_{pl}^2/\omega^2$  and take  $\omega_{pl}/\omega_p = 10^3$ ,  $\omega_{pl}$  being the plasma frequency of the metallic substrate. The parameters, as cited above, correspond to an InSb semiconductor film on a Na substrate.

Because  $\omega_{pl} \gg \omega_p$  and  $q_0 d \ll 1$ , the first term in Eq. (31), corresponding to bare metallic surface, predominates over most of the spectral range of interest. An exception occurs at the hybrid cyclotron-plasma frequency  $\omega_H$ , defined in Eq. (22). The diagonal element  $\epsilon_{zz}$  vanishes at  $\omega_H$  and from Eq. (31)  $q_z \rightarrow \infty$ . Although our perturbational approach breaks down, it is clear that a splitting occurs in the dispersion curve of the magnetopolaritons. This is shown in a narrow range in the vicinity of  $\omega_H$  in Fig. 5. At the frequencies away from  $\omega_H$ , the dispersion curve closely follows the light line ( $q_z = q_0$ ), this is because  $\omega \ll \omega_{pl}$ . We have discarded the solutions with  $q_z < q_0$ ; the reason being that these correspond to the imaginary decay constant  $\alpha_3$ . For  $\omega_{pl} \gg \omega_p$  (and  $\omega_c$ ), the correction term in the small square bracket in Eq. (31) vanishes at a frequency approximately equal to

$$\omega'_H = \left[ \omega_c^2 + \frac{\omega_p^2}{\epsilon_L - 1} \right]^{1/2}. \quad (32)$$

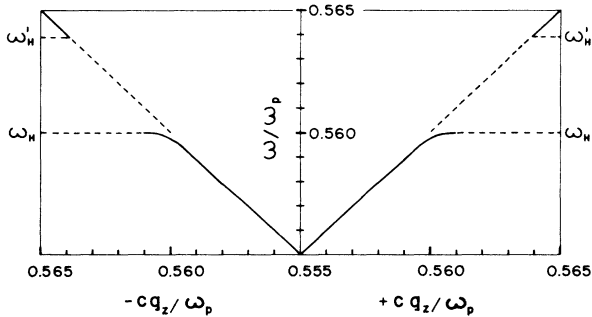


FIG. 5. The normalized frequency  $\omega/\omega_p$  vs normalized propagation constant  $cq_z/\omega_p$  for surface-plasmon polaritons modified by a semiconducting magnetoplasma overlayer. The dispersion curve has been calculated using the thin-film approximation, from Eq. (31), with  $\epsilon_3 = 1$ ,  $\epsilon_1 = 1 - \epsilon p_1^2/\omega^2$ ,  $\omega_p/\omega_{pl} = 10^{-3}$ ,  $\omega_c/\omega_p = 0.5$ ,  $\epsilon_L = 15.7$ , and  $\omega_p d/c = 2\pi \times 10^{-2}$ . This corresponds to an InSb film on a Na substrate. At the low frequencies ( $\omega \ll \omega_{pl}$ ) the curve follows closely the light line, except in the vicinity of the hybrid cyclotron-plasma frequency  $\omega_H$ . The magnetized overlayer creates a gap in the spectrum, of width  $\sim \omega_p^2/(2\epsilon_L^2\omega_H)$  just above  $\omega_H$ . Although Eq. (31) is nonreciprocal, this is hardly noticeable because of the large ratio of  $\omega_{pl}$  to  $\omega_p$ .

It may be concluded that, as a consequence of the presence of the thin film, a gap opens up in the spectrum. For  $\epsilon_L \gg 1$ , the width of the gap is

$$\omega'_H - \omega_H = \frac{\omega_p^2}{2\epsilon_L^2\omega_H}. \quad (33)$$

In the absence of  $\mathbf{B}_0$ ,  $\omega_H = \omega_p/\epsilon_L^{1/2}$  and the gap becomes  $\omega_p/2\epsilon_L^{3/2}$ .

We note that although our dispersion relation, Eq. (31), is different from the corresponding expression in the Faraday configuration, Eq. (38) in Ref. 1, the numerical results are found to be almost the same. This is because of a considerably large ratio of  $\omega_{pl}$  to  $\omega_p$ , and a pole at  $\omega = \omega_H$  in both geometries. For the same reasons the nonreciprocity, evident in Eq. (31), is hardly noticeable in Fig. 5.

### B. Magnetized film bounded by identical media

Substituting  $\epsilon_1 = \epsilon_3 = \epsilon_0$  and hence  $\alpha_1 = \alpha_3 = \alpha_0$  in the dispersion relation simplified in the TFA, Eq. (28), gives

$$2\epsilon_0\epsilon_{zz}\alpha_0 + d[\alpha_0^2(\epsilon_{zz}^2 + \epsilon_{yz}^2) + k^2\epsilon_0^2] = 0. \quad (34)$$

In this case we use the following ansatz:<sup>24</sup>

$$q_z^2 = q_0^2\epsilon_0 + K_2^2 \quad (35)$$

for a small thickness of the film. In the limit  $d \rightarrow 0$ , the film bounded by two identical dielectric media becomes a bulk characterized by the dielectric constant  $\epsilon_0$ . In this case the solution for  $q_z$  should be  $q_0(\epsilon_0)^{1/2}$ . For small but finite  $d$ , we expect that  $q_z$  will differ from  $q_0(\epsilon_0)^{1/2}$  by a small amount which is proportional to some power of  $d$ . This is the basis of our ansatz in the symmetric configuration, Eq. (35). Treating  $K_2^2$  as a very small correction and using Eq. (34), with  $\epsilon_i = \epsilon_0$  and  $\alpha_i = \alpha_0$ , we calculate  $\alpha_0$  and  $K$  (see Appendix D in Ref. 1). Substituting in Eq. (34) and neglecting the terms proportional to  $K_2^2$  and  $K_2^4$  in the coefficient of  $d$  leaves us with an expression for  $K_2$  given by

$$K_2 = -\frac{1}{2} \frac{q_0^2 d}{\epsilon_{zz}} \epsilon_0 (\epsilon_0 - \epsilon_{zz}). \quad (36)$$

Substituting  $K_2$  in Eq. (35) yields

$$q_z = q_0 \left[ \epsilon_0^{1/2} + \frac{1}{8} \frac{(q_0 d)^2}{\epsilon_{zz}^2} \epsilon_0^{3/2} (\epsilon_0 - \epsilon_{zz})^2 \right]. \quad (37)$$

Note that in the symmetric configuration in the TFA,  $q_z$  is independent of the off-diagonal element  $\epsilon_{yz}$ . We also see that in this case the dispersion relation becomes reciprocal. The necessary requirement for the validity of Eq. (37) is  $q_0 d \ll 1$ . We note that due to higher symmetry, the correction in  $q_z$  is proportional to  $d^2$ , unlike the linear  $d$  dependence in case A, Eq. (31). It may be pointed out that in the limit  $\mathbf{B}_0 = 0$ , Eq. (37) reduces exactly to the one found by Boardman and Halevi,<sup>24</sup> in the lowest order of  $d$ , for the symmetric configuration.

We have computed the dispersion relation, Eq. (37), for a finite value of  $\mathbf{B}_0$ . Apart from  $\epsilon_0 = 1.0$ , the parameters are the same as in Sec. IV A. The numerical results

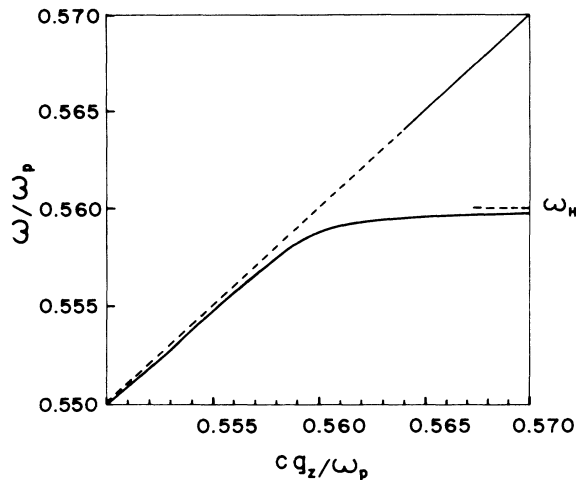


FIG. 6. The normalized frequency  $\omega/\omega_p$  vs normalized propagation constant  $cq_z/\omega_p$  for a very thin unsupported InSb film. The dispersion curve corresponds to Eq. (34). Apart from  $\epsilon_0=1.0$ , the parameters used are the same as in Fig. 5. Above  $\omega_H$  up to  $\omega'_H$  a gap of the width defined in Fig. 5 opens up in the spectrum. The dispersion relation in this case, like in Fig. 3, is reciprocal.

in terms of the dimensionless variables are shown in the vicinity of  $\omega_H$  in Fig. 6. The surface mode starts from the origin along the light line, rises towards the right of the light line, and then approaches the limit  $\omega_H$  as  $q_z \rightarrow \infty$ . Between  $\omega_H$  and  $\omega'_H$ , a gap, given by Eq. (33), opens up in the dispersion curve. This again can be ascribed due to a small but finite film thickness. For  $\omega > \omega'_H$ , the mode starts deviating towards the right of the light line with increasing  $q_z$ . However, the devia-

tion, from  $\omega'_H$  up to  $\omega_p$ , is so small that it is difficult to discern it on the scale in Fig. 6. We intend to present the detailed (exact) numerical calculations, and precise classification of the nature of the modes (surface or WG) in a forthcoming paper.<sup>25</sup>

Although Figs. 4 and 6 deal with the symmetric configuration ( $\epsilon_1=\epsilon_3=\epsilon_0=1.0$ ), they remarkably differ in the spectral range (in the  $\omega-q$  plane) that they cover. Figure 4 is applicable only for  $q_z \gg q_0$  (NR limit), far away from the light line, whereas Fig. 6 is valid for  $q_z \approx q_0$ , near the light line. In spite of these limitations and the fact that DeWames and Hall<sup>13</sup> used a set of parameters very different from ours, a coherent correspondence emerges between our Figs. 4 and 6 on one hand, and Fig. 2 of Ref. 13 on the other hand. The lower and upper modes in Fig. 4 correspond to the lowest and third-lowest *surface* (or polariton, in our terminology) modes of the above-mentioned authors; they terminate at frequencies  $\omega_{s-}$  and  $\omega_{s+}$ , respectively. The lower and the upper modes in Fig. 6 correspond to the second lowest and the uppermost *surface* modes, respectively, of DeWames and Hall; at higher frequencies both of these modes change to "bulk" or WG character (using our TFA it is not difficult to prove that  $\beta$  is imaginary quantity for  $\omega$  just below  $\omega_H$  and for  $\omega \gg \omega_H$ ). In Fig. 2 of Ref. 13 there are three additional WG modes (dashed lines). The absence of these in our Fig. 6 seems to be related to our choice of an extremely thin film. Thus we may conclude that an unsupported film in the Voigt geometry supports at least four magnetoplasma modes.

#### ACKNOWLEDGMENT

This work was supported in part by Consejo Nacional de Ciencia y Tecnología.

<sup>1</sup>M. S. Kushwaha and P. Halevi, Phys. Rev. B **35**, 3879 (1987).

<sup>2</sup>M. S. Kushwaha and P. Halevi (unpublished).

<sup>3</sup>K. W. Chiu and J. J. Quinn, Nuovo Cimento B **10**, 1 (1972).

<sup>4</sup>R. F. Wallis, J. J. Brion, E. Burstein, and A. H. Hartstein, Phys. Rev. B **9**, 3424 (1974).

<sup>5</sup>C. Uberoi and U. J. Rao, Surf. Sci. **66**, 210 (1977).

<sup>6</sup>P. Halevi and C. Guerra-Vela, Phys. Rev. B **18**, 5248 (1978).

<sup>7</sup>G. C. Aers and A. D. Boardman, J. Phys. C **11**, 945 (1978).

<sup>8</sup>P. Halevi, in *Electromagnetic Surface Modes*, edited by A. D. Boardman (Wiley, New York, 1982), p. 249.

<sup>9</sup>R. F. Wallis, in *Electromagnetic Surface Modes*, edited by A. D. Boardman (Wiley, New York, 1982), p. 575.

<sup>10</sup>T. López-Ríos, Opt. Commun. **17**, 342 (1976).

<sup>11</sup>M. Fukui, V. C. Y. So, and R. Normandin, Phys. Status Solidi B **91**, K61 (1979).

<sup>12</sup>D. Sarid, Phys. Rev. Lett. **47**, 1927 (1981).

<sup>13</sup>R. E. DeWames and W. F. Hall, Phys. Rev. Lett. **29**, 172 (1972).

<sup>14</sup>D. Sarid, Phys. Rev. B **29**, 2344 (1984).

<sup>15</sup>M. V. Ortenberg, in *Infrared and Millimeter Waves*, edited by K. J. Button (Academic, New York, 1980), p. 275.

<sup>16</sup>I. L. Tyler, B. Fisher, and R. J. Bell, Opt. Commun. **8**, 145 (1973).

<sup>17</sup>A. Hartstein and E. Burstein, Solid State Commun. **14**, 1223 (1974).

<sup>18</sup>H. Kaplan, E. D. Palik, R. Kaplan, and R. W. Gammon, J. Opt. Soc. Am. **64**, 1551 (1974).

<sup>19</sup>V. S. Ambrazeviciene and R. S. Brazis, Solid State Commun. **18**, 415 (1976).

<sup>20</sup>P. K. Tien, Rev. Mod. Phys. **49**, 361 (1977).

<sup>21</sup>R. W. Alexander, Jr., R. J. Bell, and C. A. Ward, in *Electromagnetic Surface Modes*, edited by A. D. Boardman (Wiley, New York, 1982), p. 201.

<sup>22</sup>K. L. Kliever and R. Fuchs, Adv. Chem. Phys. **27**, 355 (1974).

<sup>23</sup>The effective mass of an electron in a metal is 2 orders of magnitude greater than that in a semiconductor like InSb. For this reason the cyclotron frequency of the metal is negligible and hence the magnetoplasma may be restricted to the semiconductor film.

<sup>24</sup>A. D. Boardman and P. Halevi (unpublished).

<sup>25</sup>M. S. Kushwaha and P. Halevi (unpublished).